Preprint Number : IITM/PH/TH/2007/6

Classical bifurcations and entanglement in smooth Hamiltonian system

M. S. Santhanam[1], V. B. Sheorey[1] and Arul Lakshminarayan[2*]
[1] *Physical Research Laboratory, Navrangpura, Ahmedabad 380 009, India.*
[2] *Max Planck Institute for the Physics of Complex Systems, Nöthnitzer Strasse 38., Dresden 01187, Germany*
(Dated: June 30, 2007)

We study entanglement in two coupled quartic oscillators. It is shown that the entanglement, as measured by the von Neumann entropy, increases with the classical chaos parameter for generic chaotic eigenstates. We consider certain isolated periodic orbits whose bifurcation sequence affects a class of quantum eigenstates, called the channel localized states. For these states, the entanglement is a local minima in the vicinity of a pitchfork bifurcation but is a local maxima near a anti-pitchfork bifurcation. We place these results in the context of the close connections that may exist between entanglement measures and conventional measures of localization that have been much studied in quantum chaos and elsewhere. We also point to an interesting near-degeneracy that arises in the spectrum of reduced density matrices of certain states as an interplay of localization and symmetry.

PACS numbers: 05.45.-a, 03.67.Mn, 05.45.Mt

I. INTRODUCTION

The study of entanglement is currently an active area of research in view of it being a physical resource for quantum information theory, quantum computing, quantum cryptography and teleportation [1]. At a classical level, entanglement does not have a corresponding counterpart. However, increasingly it is being realized that the nature of classical dynamics, whether it is regular or chaotic, affects entanglement in the quantized version of the system [2]. In general, larger chaos in the system leads to larger entanglement production. This has been established by considering kicked top models [3], bakers map [4], Dicke model [5], billiard in a magnetic field [6], kicked Bose-Einstein condensates [7] and N-atom Jaynes-Cummings model [8]. In contrast to these studies, the role of classical bifurcations in entanglement of chaotic systems has not received much attention. Even though entanglement is a purely quantum attribute, it is nevertheless affected by the qualitative nature of the dynamics in phase space. The results to this effect are obtained primarily in the context of quantum phase transitions in the ground state of infinite systems in which the entanglement is maximal at critical parameter values [12]. For instance, for case of ions driven by laser fields and coupled to a heat bath, i.e, a form of Dicke model was shown to exhibit maximal entanglement of its ground state at the parameter value at which classical system bifurcates. Similar result for the ground state was reported from the study of coupled tops, a generalization of the two dimensional transverse field quantum Ising model [9] as well from Jahn-Teller models [10]. The ground state entanglement of mono-mode Dicke model is shown to be related to Hopf bifurcation [11]. Qualitatively similar results for two component Bose-Einstein condensate are also known [13]. In all these cases, the treatment is confined mostly to the ground state of the system that exhibits criticality and involves one single classical bifurcation.

Do these results hold good for chaotic, smooth Hamiltonian systems that do not exhibit criticality in the sense of phase transitions ? As opposed to a single bifurcation, what happens in bifurcation sequences where stability loss and stability gain interleave one another ? Both these questions explore the connection between chaos and entanglement in a physical setting that is different from the earlier studies. In the context of this work, we examine a Hamiltonian system whose classical dynamics is controlled by a single tunable parameter. The changes in the parameter leads to changes in the phase space structure; for instance regularity to chaos transition and bifurcation sequences of fixed points. Typically, chaotic systems display a sequence of bifurcations. Consider, for instance, the coupled oscillator systems, a paradigm of chaos for smooth Hamiltonian systems and is related to atoms in strong magnetic fields, the quadratic Zeeman effect problems [14]. In these cases, one particular sequence of bifurcation is a series of pitchfork and anti-pitchfork bifurcations [15]. The pitchfork corresponds to a periodic orbit losing stability and in the Poincarè section this appears as a elliptic fixed point giving way to a hyperbolic fixed point. The anti-pitchfork is when the periodic orbit gains stability. In this work, we consider coupled quartic oscillators and show that the entanglement in the highly excited states of the system is modulated by classical bifurcations. We could place this in the context of works that lend support to the notion that for generic one-particle states there is a strong correlation between entanglement and measures of localization [16, 17, 18].

*Permanent address: Department of Physics, Indian Institute of Technology Madras, Chennai, 600036, India.

II. ENTANGLEMENT IN A BIPARTITE SYSTEM

A pure quantum state $|\Psi\rangle$ composed of many subsystems $|\phi_i\rangle$ is said to be entangled if it cannot be written down as a direct product of states corresponding to each of the subsystem.

$$|\Psi\rangle_{\text{entangled}} \quad \neq \quad |\phi_1\rangle \otimes |\phi_2\rangle \otimes |\phi_3\rangle ..... \otimes |\phi_n\rangle \quad (1)$$

Thus, entanglement implies stronger than classical correlations. If $\rho = |\psi\rangle\langle\psi|$ is the density matrix representation for a pure state $|\psi\rangle$, then the reduced density matrix (RDM) can be obtained by applying the trace operation to one of the degrees of freedom. Thus,

$$\rho_1 = \text{Tr}_2|\psi\rangle\langle\psi| \qquad \rho_2 = \text{Tr}_1|\psi\rangle\langle\psi| \quad (2)$$

are two RDMs, whose one of the degrees of freedom is traced out. The notation Tr_i denotes that the trace operation is applied on the ith degree of freedom. Schmidt decomposition [1] provides a representation for $|\psi\rangle$ in terms of product of basis states,

$$|\psi\rangle = \sum_{i=1}^{N} \sqrt{\lambda_i} \;\; |\phi_i\rangle_{(1)} \;\; |\phi_i\rangle_{(2)} \quad (3)$$

where $|\phi_i\rangle_{(1)}$ and $|\phi_i\rangle_{(2)}$ are the eigenvectors of the RDMs ρ_1 and ρ_2 respectively, and λ_i are the eigenvalues of either of the RDMs. The von Neumann or the entanglement entropy of pure state is given by,

$$S = -\sum_{i=1}^{N} \lambda_i \log \lambda_i \quad (4)$$

Thus, when $S = 0$, the subsystems are not entangled and when $S > 0$, they are entangled. The Schmidt decomposition provides a compact and unique representation for the given eigenstate (unique in the generic case when the non-zero spectrum of the RDM is nondegenerate).

III. HAMILTONIAN MODEL AND BIFURCATION SEQUENCE

A. Quartic oscillator

We consider the Hamiltonian system given by,

$$H = p_x^2 + p_y^2 + x^4 + y^4 + \alpha x^2 y^2 \quad (5)$$

with α being the tunable chaos parameter. For $\alpha = 0, 2, 6$, the system is classically integrable and becomes predominantly chaotic as $\alpha \to \infty$. This has been extensively studied as a model for classical and quantum chaos in smooth Hamiltonian systems [19] and exhibits qualitatively similar dynamics as the host of problems involving atoms in strong external fields. In the limit $\alpha \to \infty$, it is also of relavance as model of classical Yang-Mills field [20]. To study the quantum analogue of this system, we quantize it in a symmetrized basis set given by,

$$\psi_{n_1,n_2}(x,y) = \mathcal{N}(n_1,n_2)\left[\phi_{n_1}(x)\phi_{n_2}(y) + \phi_{n_2}(x)\phi_{n_1}(y)\right] \quad (6)$$

where $\mathcal{N}(n_1, n_2)$ is the normalization constant and $\phi(x)\phi(y)$ is the eigenstate of unperturbed quartic oscillator with $\alpha = 0$. The choice of this form of basis set is dictated by the fact that the quartic oscillator has C_{4v} point group symmetry, i.e., all the invariant transformations of a square. Hence we have chosen the symmetry adapted basis sets as in Eq. 6 from A_1 representation of C_{4v} point group.

Thus, the nth eigenstate is,

$$\Psi_n(x,y) = \sum_{j(n_1,n_2)=1} a_{n,j(n_1,n_2)} \; \psi_{n_1,n_2}(x,y) \quad (7)$$

where $a_{n,j(n_1,n_2)} = \langle\psi(x,y)|\Psi_n(x,y)\rangle$ are the expansion coefficients in the unperturbed basis space. Note that n_1, n_2 are even integers and $a_{n,j(n_1,n_2)} = a_{n,j(n_2,n_1)}$ in A_1 representation of C_{4v} point group. The eigenvalue equation is solved numerically by setting up Hamiltonian matrices of order 12880 using 160 even one-dimensional basis states.

B. Bifurcation sequence in quartic oscillator

In a general chaotic system many bifurcation sequences are possible. However, a two dimensional Hamiltonian system can exhibit only five types of bifurcations [15]. One such prominent sequence is a series of pitchfork and anti-pitchfork bifurcation shown schematically in Fig 1. To reiterate, a pitchfork bifurcation takes place when a stable orbit loses stability and gives rise to two stable orbits. Anti-pitchfork bifurcations happen when a stable orbit is spontaneously born due to the merger of two unstable orbits. We will focus on a particular periodic orbit, referred to as the channel orbit in the literature [21], given by the initial conditions $\{x, y = 0, p_x, p_y = 0\}$, which displays such a bifurcation sequence. The Poincaré section in the vicinity of the channel orbit has interesting scaling properties and the orbit itself has profound influence on a series of quantum eigenstates, called localized states, in the form of density enhancements or scars [22]. Such density enhancements due to channel orbits have also been noted in atoms in strong magnetic fields or the diamagnetic Kepler problem [23] as well.

The stability of the channel orbit in the quartic oscillator in Eq (5) is indicated by the trace of monodromy matrix $J(\alpha)$ obtained from linear stability analysis. It can be analytically obtained for the channel orbits [24] as,

$$\text{Tr } J(\alpha) = 2\sqrt{2}\cos\left(\frac{\pi}{4}\sqrt{1+4\alpha}\right). \quad (8)$$

The channel orbit is stable as long as $|\text{Tr}J(\alpha)| < 2$ and it undergoes bifurcations whenever $\text{Tr}J(\alpha) = \pm 2$. From

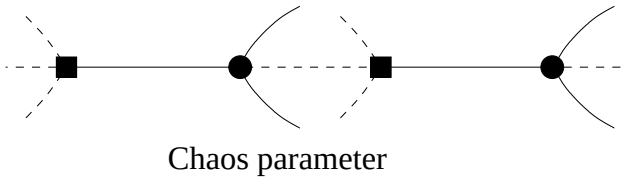

FIG. 1: The schematic of a typical bifurcation sequence involving a series of pitchfork (circles) and anti-pitchfork (square) bifurcations as a function of chaos parameter. The solid lines indicate that the orbit is stable and dashed line indicate instability.

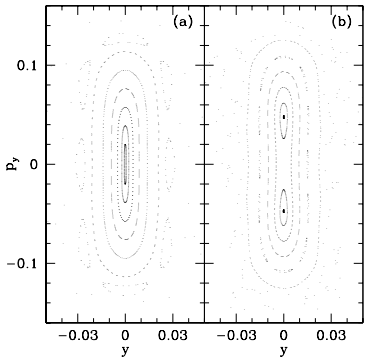

FIG. 2: The Poincare section for the quartic oscillator in Eq. 5 in shown for (a) $\alpha = 90$ and (b) $\alpha = 90.5$. Note that at $\alpha = 90$ the periodic orbit undergoes a pitchfork bifurcation.

this condition, it is clear that the bifurcations take place at $\alpha_n = n(n+1)$, $(n = 1, 2, 3....)$. Thus the channel orbit undergoes an infinite sequence of pitchfork and anti-pitchfork bifurcations at $\alpha = \alpha_n$. Note that for $n = 9$, we have $\alpha = 90$ as one of the pitchfork bifurcation points. The Poincaré sections displayed in Fig 2 shows that the stable channel orbit at $\alpha = 90$ (Fig 2(a)) bifurcates and gives birth to two new stable orbits (Fig 2(b)) while the channel orbit itself becomes unstable. Thus, pitchfork bifurcations take place at $\alpha_n = 2, 12, 30, 56, 90, ...$ and anti-pitchfork at $\alpha_n = 6, 20, 42, 72, ...$ This can be observed in the plot of $\mathrm{Tr}J(\alpha)$ as a function of α shown in Fig 3.

IV. QUARTIC OSCILLATOR STATES AND REDUCED DENSITY MATRIX

A. Quartic oscillator spectra

The quantum spectrum of the quartic oscillator is extensively studied and reported [19, 22, 28]. For the purposes of this study, we note that two classes of eigenstates can be identified. The first one is what we call a generic state whose probability density $|\Psi_n(x, y)|^2$ covers the entire accessible configuration space. Most of the eigenstates fall in this class and they are instances of

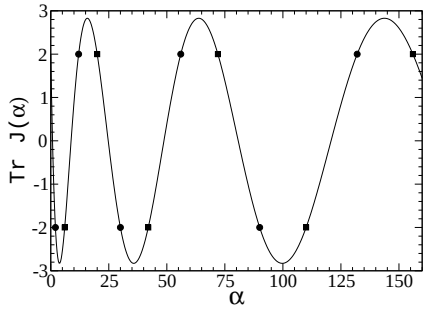

FIG. 3: The linear stability of the channel orbit as a function of α. The orbit is stable for $|\mathrm{Tr}\ J(\alpha)| < 2$. The pitchfork bifurcation points are indicated by circles and anti-pitchfork bifurcations are indicated by squares.

Berry's hypothesis that the Wigner function of a typical chaotic state condenses on the energy shell [25]. In Fig 4(a), we show the expansion coefficients for the 1973rd eigenstate of the quartic oscillator counted sequentially from the ground state for $\alpha = 90$. Notice that the state is delocalized over a large set of basis states. These class of states are well described by random matrix theory. The second class of states is the localized states, which has enhanced probability density in the vicinity of the underlying classical periodic orbits. Theoretical support for this class of states based on semiclassical arguments is obtained from the works of Heller [26], Bogomolny and Berry [27]. As a typical case, Fig 4(b) shows the expansion coefficients for the 1972nd state which is localized over very few basis states in contrast to the one in Fig 4(a). In this work, we concentrate on a subset of such eigenstates whose probability density is concentrated in the vicinity of the channel periodic orbit. This set of states are nearly separable and can be approximately labelled by a doublet of quantum numbers $(N, 0)$ using the framework of adiabatic theory [22, 28]. Note that such a labeling is not possible for the generic states since they are spread over a large number of basis states.

B. Reduced density matrix

In this section, we compute the eigenvalues of the RDM and the entanglement entropy of the quartic oscillator eigenstates as a function of the chaos parameter α. In terms of the expansion coefficients in Eq. (7), the elements of RDM, $\mathbf{R}_x$, can be written down as,

$$\langle n_2|\rho^{(x)}|n_2'\rangle = \sum_{n_1=1}^{M} K_{n_1,n_2} a_{n_1,n_2} a_{n_1,n_2'}, \qquad (9)$$

where the normalization constant $K_{n_1,n_2} = 1$ if $n_1 = n_2$ and $= 1/2$ if $n_1 \neq n_2$. In this case, the y-subsystem has been traced out. Similarly another RDM, $\mathbf{R}_y$, with elements $\langle n_2|\rho^{(y)}|n_2'\rangle$ can be obtained by tracing over x variables. Let $\mathbf{A}$ represent the eigenvector matrix of order $(M+2)/2$ with elements a_{n_1,n_2}, where

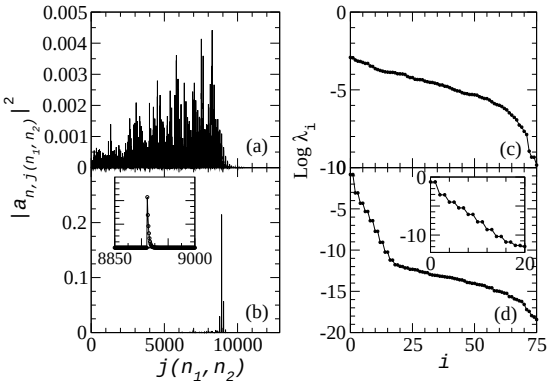

FIG. 4: Quartic oscillator eigenstates for $\alpha = 90$ in the unperturbed basis. (a) 1973rd state (delocalized), (b) 1972nd state (localized). The inset is the magnification of the dominant peak. The eigenvalues of the RDMs for (c) 1973rd state and (d) 1972nd state. The inset in (d) is the magnification of the dominant eigenvalues that display degeracy.

$n_1, n_2 = 0, 2, 4....M$ labels the rows and columns respectively. Then, in matrix language, the RDM $\mathbf{R}_x = \mathbf{A^T A}$ is matrix of order $(M+2)/2$.

In our case, $M = 318$ and we numerically diagonalize the RDM of order 160. The eigenvalues of RDM for a typical delocalized state and a localized state is plotted in Fig 4(c,d). In general, the dominant eigenvalues fall exponentially, though with different rates, for both the generic and typical localized state indicating that the Schmidt decomposition provides a compact representation for the given eigenstate. Earlier such a behavior was noted for coupled standard maps [2]. The first few dominant eigenvalues of RDM for localized states display (near-)degeneracy (see Fig 4(d)). This arises as a consequence of (i) C_{4v} symmetry of the potential due to which the eigenvector matrix is symmetric, i.e, $a_{n_1,n_2} = a_{n_2,n_1}$ and (ii) the localization is exponential in the direction perpendicular to that in which the quanta of excitation is larger [28], i.e, $a_{N,n_2} \propto \exp(-\omega n_2)$, where $\omega > 0$ is a constant independent of N.

The origin of near-degeneracy can be understood by by considering a simple model of 4×4 symmetric eigenvector matrix (the state number index n is suppressed such that $a_{n,j(n_1,n_2)} = a_{n_1,n_2}$),

$$\mathbf{P} = \begin{pmatrix} a_{0,0} & a_{2,0} & a_{N,0} & a_{N+2,0} \\ a_{2,0} & a_{2,2} & a_{N,2} & a_{N+2,2} \\ a_{N,0} & a_{N,2} & a_{N,N} & a_{N+2,N} \\ a_{N+2,0} & a_{N+2,2} & a_{N+2,N} & a_{N+2,N+2} \end{pmatrix}. \quad (10)$$

Here we have only used the one-dimensional quartic oscillator quantum numbers $(0, 2, N, N+2)$ because the localized states can be approximately well represented by all possible doublets arising from these quantum numbers. For instance, an adiabatic separation with the $(N, 0)$ manifold gives a good estimate for the energy of its localized states [28]. The representation gets better as we add more 1D quantum numbers to the list above.

The exponential localization implies that $a_{n_1,n_2} \approx 0$ for $n_1 \sim n_2$. Further, $a_{n_1,n_2} \approx 0$ if $n_1, n_2 << N$. Thus, elements $a_{N,N} \sim a_{N+2,N} \sim a_{N+2,N+2} \sim a_{0,0} \approx 0$. Then, we can identify a block matrix B with non-zero elements as,

$$\mathbf{B} = \begin{pmatrix} a_{N,0} & a_{N+2,0} \\ a_{N,2} & a_{N+2,2} \end{pmatrix} \quad (11)$$

Then, the eigenvector matrix $\mathbf{P}$ can be approximated as,

$$\mathbf{P} \approx \begin{pmatrix} \mathbf{0} & \mathbf{B} \\ \mathbf{B^T} & \mathbf{0} \end{pmatrix}. \quad (12)$$

Under the conditions assumed above, the RDM separates into two blocks which are transpose of one another. Thus, the reduced density matrix will have the form,

$$\mathbf{R} = \mathbf{P^T P} = \begin{pmatrix} \mathbf{BB^T} & \mathbf{0} \\ \mathbf{0} & \mathbf{B^T B} \end{pmatrix} \quad (13)$$

Since the eigenvalues remain invariant under transposition of a matrix, *i.e*, the eigenvalues of $\mathbf{BB^T}$ and $\mathbf{B^T B}$ are identical and hence we obtain the degeneracy. Though we use a 4×4 matrix to illustrate the idea, this near degeneracy would arise for any eigenvector matrix of even order, if the symmetry and exponential decay conditions are satisfied.

For the localized state shown in Fig 4(b), $N = 264$ and the dominant eigenvalue of RDM using the approximate scheme in Eqns (10-13), is $\lambda_1 = 0.4434$. This is doubly degenerate and compares favorably with the exact numerical result of 0.4329. As observed in Fig 4(d), the degeneracy breaks down as we travel down the index. As pointed out, the dominant eigenvalues of RDM correspond to definite 1D quantum oscillator modes that exhibit exponential decay in the perpendicular mode. This is not true of all the oscillator modes and hence the degeneracy is broken.

C. Entanglement entropy

Entanglement entropy for each eigenstate is computed from the eigenvalues of the RDM using Eq (4). In Fig 5, we show the entanglement entropy of the quartic oscillator at $\alpha = 30$ for one thousand eigenstates starting from the ground state. The localized states have values of entanglement entropy much lower than the local average as seen from the dips in the figure. Most of them are much closer to zero and substantiate the fact that they are nearly separable states. In the next section we will show that the entanglement entropy of localized state is modulated by the bifurcation in the underlying channel periodic orbit.

The generic delocalized states, on the other hand, form the background envelope seen in Fig 5. These chaotic states are not affected by the bifurcations in the isolated orbits. It is known that such delocalized states can

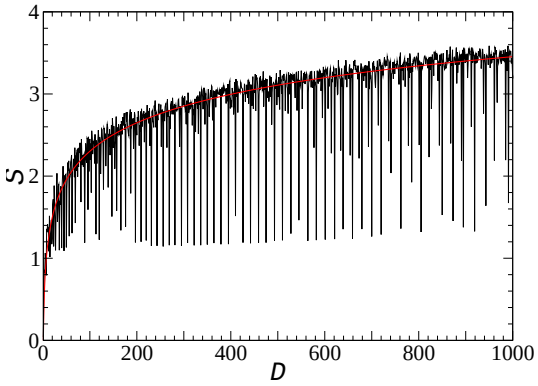

FIG. 5: (Color Online) Entanglement entropy for the quartic oscillator at $\alpha = 30$ from ground state to 1000th state. The localized states have lower value of entanglement entropy as seen from the dips in the curve. The solid red curve is S_{RMT}, the RMT average of entanglement entropy.

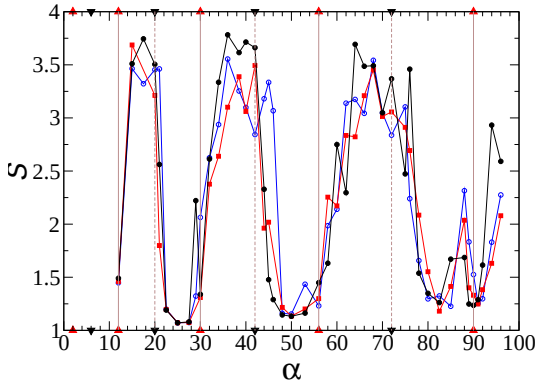

FIG. 6: (Color Online) Entanglement entropy as a function of α. The three curves correspond to different $(N, 0)$ type localized states; solid circles (240,0), open circles (200,0) and squares (210,0). The positions of pitchfork bifurcations (triangle up) and anti-pitchfork bifurcations (triangle down) are marked on both the x-axes.

be modeled using random matrix theory and hence the distribution of their eigenvectors follows Porter-Thomas distribution [29]. The entanglement entropy can also be calculated based on RMT assumptions and it is known to be [30], $S_{RMT} = \ln(\gamma M)$ where $\gamma \approx 1/\sqrt{e}$ and M is the dimensionality of the reduced density matrix. In the case of quartic oscillator, the Hilbert space is infinite in dimension and we take M to be the effective dimension M_{eff} of the RDM. One indicator of the effective dimension of the state is the inverse participation ratio of the eigenstates. Based on this measure and due to C_{4v} symmetry of the quartic oscillator, we have $M_{eff}^2 = D$ where D is the state number. Thus, the effective dimension of RDM is, $M_{eff} = \sqrt{D}$. Finally, we get for the entanglement entropy,

$$S_{RMT} = \ln(\gamma M_{eff}) \sim \ln(\gamma\sqrt{D}). \tag{14}$$

In Fig 5, S_{RMT} is shown as solid red curve and it correctly reproduces the envelope formed by the delocalized states while the localized states stand out as deviations from RMT based result, namely, S_{RMT}.

V. ENTANGLEMENT ENTROPY AND BIFURCATIONS

In this section, we show the central result of the paper that the entanglement entropy is a minimum at the points at which the underlying periodic orbit undergoes a pitchfork bifurcation. As pointed out before, the localized states of the quartic oscillator are characterized by the doublet $(N, 0)$ and are influenced by the channel periodic orbit. We choose a given localized state, say, with $N = 200$ and compute the entanglement of the same state, i.e, $(200, 0)$ state as a function of α. The state that can be characterized by the doublet $(200, 0)$ will be a localized state at every value of α. The result is shown in Fig 6 as the curve plotted with open circles. The values of α at which the pitchfork and anti-pitchfork bifurcation takes is marked in both the horizontal axes of the figure as triangle-up and triangle-down respectively. For the purpose of easier visualization, they are connected by vertical lines. Notice that the entanglement entropy attains a local minima in the vicinity of every classical pitchfork bifurcation and it attains a local maxima near every anti-pitchfork bifurcation. As Fig 6 shows, similar result is obtained for two different localized states with $(N = 210, 0)$ and $(N = 240, 0)$. All these localized states are in the energy regime of highly excited states where the classical system is predominantly chaotic. The striking similarity between the classical stability curve for a particular periodic orbit, namely the channel orbit, in Fig. (3) and the variation of the entanglement of the localized state is to be noted. We have also numerically verified (not shown here) that a similar result is obtained in the case of another potential where pitchfork and anti-pitchfork bifurcations of the channel periodic orbit play an important role, namely, in $V(x, y) = x^2 + y^2 + \beta x^2 y^2$, where β is the chaos parameter.

At a pitchfork bifurcation, as shown in Fig. 2, the fixed point corresponding to the channel periodic orbit loses stability and becomes a hyperbolic point. The central elliptic island seen in Fig 2(a), breaks up into two islands. The localized state that mainly derives its support from the classical structures surrounding the stable fixed point suffers some amount of delocalization, but is largely supported by the stable regions. At an anti-pitchfork bifurcation, the hyperbolic point becomes an elliptic fixed point and the orbit has gained stability and a small elliptic island just comes into existence. Hence, the eigenstate is still largely delocalized since the small elliptic island is insufficient to support it. This heuristic picture which is quite sufficient to explain oscillations in localization measures is seen to be surprisingly valid even for the somewhat less intuitive measure of entanglement.

It has been noted earlier that when the corresponding classical system undergoes a pitchfork bifurcation, the entanglement entropy defined by Eq (4) attains a *maximum* [9], and it has been conjectured to be a generic property. We note that this, apparently contradictory result, is however in the context of an equilibrium point undergoing a bifurcation and the relevant state is the ground state, whereas in the case we are studying here the orbit that is bifurcating is a periodic orbit and the states are all highly excited. In this situation there is a much tighter correlation between more conventional measures of localization (Shannon entropy, participation ratio etc.) and entanglement.

As the parameter α is increased, the quartic oscillator gets to be predominantly chaotic and this should imply increase in entanglement. However, this is true only for the generic delocalized states as seen in Fig 5. The localized states are influenced not so much by the increasing volume of chaotic sea but by the specific periodic orbits that underlie them. Hence, for these states, it is only to be expected that the qualitative changes in the phase space in the vicinity of the corresponding periodic orbits affect quantum eigenstate and hence its entanglement as well. This can be expected to be a generic feature of entanglement in quantum eigenstates of mixed systems.

VI. CONCLUSIONS

In summary, we considered a smooth Hamiltonian, namely the two-dimensional, coupled quartic oscillator as a bipartite system. We study the effect of classical bifurcations on the entanglement of its quantum eigenstates. The quartic oscillator is a classically chaotic system. One particular class of eigenstates of the quartic oscillator, the localized states are scarred by the channel periodic orbits. We have shown that the entanglement entropy of these localized states is modulated by the bifurcations in the underlying channel periodic orbit. When this orbit undergoes a pitchfork bifurcation, the entanglement attains a local minimum and iwhen it undergoes an anti-pitchfork bifurcation the entanglement is a local maximum. Physically, this is related to the presence or the absence of elliptic islands in the phase space in the vicinity of the channel orbit. We expect this to be a general feature of bipartite quantum systems whose classical analogue display bifurcation features.

Acknowledgments

We thank J. N. Bandyopadhyay for discussions and comments.

[1] M. A. Nielsen and I. L. Chuang, *Quantum Computation and Quantum Information* (Cambridge University Press, Cambridge, 2000).
[2] A. Lakshminarayan, Phys. Rev. E **64**, 036207 (2001); K. Furuya1, M. C. Nemes, and G. Q. Pellegrino, Phys. Rev. Lett. **80** 5524 (1998); X. Wang, Shohini Ghose, Barry C. Sanders and Bambi Hu, Phys. Rev. E **70**, 016217 (2004); C. Mejia-Monasterio, G. Benenti, G. G. Carlo, G. Casati, Phys. Rev. A **71** 062324 (2005).
[3] H. Fujisaki, T. Miyadera and A. Tanaka, Phys. Rev. E **67**, 066201 (2003); J. N. Bandyopadhyay and A. Lakshminarayan, Phys. Rev. E **69**, 016201 (2004).
[4] A. J. Scott and C. M. Caves, J. Phys. A **36**, 9553 (2003).
[5] Xi-Wen Hou and Bambi Hu, Phys. Rev. A **69**, 042110 (2004).
[6] Marcel Novaes and Marcus A. M. de Aguiar, Phys. Rev. E **70**, 045201(R) (2004).
[7] Q. Xie and W. Hai, Eur. Phys. J. **33D**, 265 (2005).
[8] R. M. Angelo, K. Furuya, M. C. Nemes, and G. Q. Pellegrino, Phys. Rev. A **64**, 043801 (2001);
[9] A. P. Hines, R. H. McKenzie and G. J. Milburn, Phys. Rev. A **71** , 042303 (2005).
[10] A. P. Hines, C. M. Dawson, R. H. McKenzie and G. J. Milburn, Phys. Rev. A **70**, 022303 (2004).
[11] M. C. Nemes *et al.*, Phys. Lett. A **354**, 60 (2006).
[12] T. Osborne and M. Nielsen, Phys. Rev. A **66**, 032110 (2002); A. Osterloh *et al.,* Nature **416**, 608 (2002).
[13] Q. Xie and W. Hai, Eur. Phys. J. **39D**, 277 (2006).
[14] H. Friedrich and D. Wintgen, Phys. Rep. **183**, 37 (1989).
[15] J.-M. Mao and J. B. Delos, Phys. Rev. A **45**, 1746 (1992).
[16] A. Lakshminarayan, V. Subrahmanyam, Phys. Rev. A **67**, 052304 (2003).
[17] H. Li, X. Wang, and B. Hu, J. Phys. A:Math. Gen. **37**, 10665 (2004).
[18] H. Li and X. Wang, Mod. Phys. Lett. B **19**, 517 (2005).
[19] O. Bohigas, S. Tomsovic and D. Ullmo, Phys. Rep. **233**, 45 (1993).
[20] W.-H. Steeb, J. A. Louw and C. M. Villet, Phys. Rev. D **33**, 1174 (1986); A. Carnegie and I. C. Percival, J. Phys. A **17**, 801 (1984).
[21] K. M. Atkins and G. S. Ezra, Phys. Rev. A **50**, 93 (1994).
[22] B. Eckhardt, Phys. Rev. A **39**, 3776 (1989); J. Zakrzewski and R. Marcinek, Phys. Rev. A **42**, 7172 (1990).
[23] K. Muller and D. Wintgen, J. Phys. B **27**, 2693 (1994); D. Delande and J. C. Gay, Phys. Rev. Lett. **59**, 1809 (1987).
[24] H. Yoshida, Cell. Mech. **31**, 363 (1983); Physica **29D**, 128 (1987).
[25] M. V. Berry
[26] E. J. Heller, Phys. Rev. Lett. **53**, 1515 (1984); in *Les*

Houches LII, Chaos and Quantum Physics, edited by M.-J. Giannoni, A. Voros, and J. Zinn-Justin, (North-Holland, Amsterdam, 1991).

[27] M. V. Berry, Proc. R. Soc. Lond. A **423**, 219 (1989); E. B. Bogomolny, Physica D **31**, 169 (1988).

[28] M. S. Santhanam, V. B. Sheorey and A. Lakshminarayan, Phys. Rev. E **57**, 345 (1998).

[29] F. Haake, *Quantum Signatures of Chaos*, (Springer-Verlag, Berlin, 2000).

[30] J. N. Bandyopadhyay and A. Lakshminarayan, Phys. Rev. Lett. **89**, 060402 (2002).